Antibody-Catalyzed Removal of the *p*-Nitrobenzyl Ester Protecting Group: The Molecular Basis of Broad Substrate Specificity

Shinwa Kurihara, Takeshi Tsumuraya, Kayo Suzuki, Masataka Kuroda, Lidong Liu, Yumiko Takaoka, and Ikuo Fujii*[a]

Abstract: Antibody catalysts for the removal of the *p*-nitrobenzyl ester protecting group have been generated to accommodate a broad range of substrates. Antibody 7B9, which was elicited against *p*-nitrobenzyl phosphonate **1**, catalyzed the hydrolyses of *p*-nitrobenzyl monoesters of nonsubstituted, and β- and γ-substituted glutaric acids with almost identical K_m and k_{cat} values. In addition, 7B9 displayed substrate tolerance towards the α-substituents and accepted the *p*-nitrobenzyl esters of Leu, Norleu, and Phe. To define the molecular basis of the broad substrate tolerance, we have cloned and sequenced the antibody and constructed a model of the active-site – hapten complex. The model showed a relatively shallow pocket of the antigen-combining site that accommodates the *p*-nitrobenzyl moiety, and this is consistent with the observed substrate specificity. Thus, in the antibody-catalyzed reaction, the α-, β-, and γ-substituents of the substrates should be outside the combining site and ignored by the antibody recognition. A structural comparison of 7B9 with antibody D2.3, elicited against the structurally similar haptenic phosphonate, suggests the significance of the linker moiety in hapten design, which endows antibody catalysts with broad substrate specificity. These investigations provide new strategies for the generation of catalytic antibodies that accept a broad range of substrates for practical applications in organic synthetic chemistry.

Keywords: catalytic antibodies · hapten · immunization · protecting groups · transition states

Introduction

Catalytic antibody technology, based on the enormous diversity of the immune system, is the most potent method available for the generation of novel protein catalysts that can facilitate a considerable number of different chemical transformations.[1] The antibody-catalyzed reactions proceed by a highly regio/stereoselective mode, according to the reaction pathway programmed in the hapten. This is beneficial for the development of new methods for organic synthetic chemistry. However, due to the inherent binding properties of antibodies, the substrate specificity is still very restricted. For practical uses, catalytic antibodies must be applicable to a wide range of substrates. There have been a number of attempts to endow catalytic antibodies with broad substrate specificity.[2] In previous reports, we have described catalytic antibodies that catalyze the regioselective deprotection of a variety of acylated carbohydrates[2a] and the enantioselective hydrolysis of amino acid esters,[2b] and other groups have presented antibody-catalyzed chemoselective reactions with various substrates.[2c, d] Although some haptenic strategies have been proposed to give catalytic antibodies with broad substrate specificity, investigations of the produced immunoglobulin proteins have resulted in only a limited understanding of the antigen-binding site structures and the catalytic functions. In this work to discuss the molecular basis of the broad substrate specificity, we have generated catalytic antibodies that hydrolyze a wide variety of *p*-nitrobenzyl esters and constructed a three-dimensional model of the antigen-combining site. These investigations provide new strategies for the generation of catalytic antibodies for practical applications in organic synthetic chemistry.

In view of the mild reaction conditions and the strict selectivity of antibody-catalyzed reactions, the removal of protecting groups seems to be most beneficial for organic synthetic chemistry.[2a–c, 3] Therefore, we have focused on an antibody-catalyzed deprotection of *p*-nitrobenzyl esters, which are frequently found in syntheses of natural products, drugs, and other organic compounds. The benzyl groups, such as *p*-nitrobenzyl and *p*-methoxybenzyl, form a cluster of the most general protective groups for carboxyl functions[4] due to the selectivity of their removal and their relative stability to most acidic and basic reaction conditions; in peptide synthesis,

[a] Dr. I. Fujii, S. Kurihara, Dr. T. Tsumuraya, K. Suzuki, Dr. M. Kuroda, Dr. L. Liu, Y. Takaoka
Department of Bioorganic Chemistry
Biomolecular Engineering Research Institute
6-2-3 Furuedai, Suita, Osaka, 565-0874 (Japan)
Fax: (+81) 6-6872-8219
E-mail: fujii@beri.co.jp

0947-6539/00/0609-1656 $ 17.50+.50/0

they are used complimentarily along with the acid-sensitive Boc group. Catalytic hydrogenolysis has also been used for selective removal. However, sulfur-containing compounds, such as azetidinone antibiotics, have a "poisoning" effect on hydrogenation catalysts (Pd/carbon) and result in the use of a large quantity of the catalyst[5] and low yields. These facts have stimulated us to develop deprotecting methods for *p*-nitrobenzyl esters with antibody catalysts.

Results and Discussion

Design and synthesis of the hapten: A haptenic phosphonate transition-state analogue **1** (Scheme 1) was designed to generate catalytic antibodies that hydrolyze *p*-nitrobenzyl ester derivatives (Figure 1). To induce broad substrate acceptance in an antibody-catalyzed reaction, we have used a haptenic

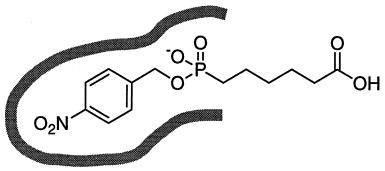

Figure 1. Schematic drawing of an antibody-combining site complexed with hapten **1**.

strategy similar to that proposed by Janda et al.[2c] The hapten **1** was composed of two different immunogenic regions, a strongly immunogenic *p*-nitrophenyl ring and a nonimmunogenic unsubstituted alkyl chain, and was conjugated to the carrier proteins with the alkyl chain for use as an antigen. Consequently, the hapten might give antibodies that strongly recognize the *p*-nitrobenzyl phosphonate moiety but not the alkyl chain.

Diethyl phosphonate **2** (Scheme 1), which was prepared by the Arbuzov reaction between triethyl phosphite and ethyl 6-bromohexanoate, was treated with hydrochloric acid and then coupled with *p*-nitrobenzyl alcohol to give the tri-*p*-nitrobenzyl ester **3**. Hydrolysis of the ester groups afforded hapten **1**. Finally, hapten **1** was conjugated to the carrier proteins, keyhole limpet hemocyanin (KLH) and bovine serum albumin (BSA), by means of a conventional *N*-hydroxysuccinimide (NHS) activated ester method (Scheme 1). The protein conjugate KLH-**1** was used for immunization, and BSA-**1** was used for an enzyme-linked immunosorbent assay (ELISA).

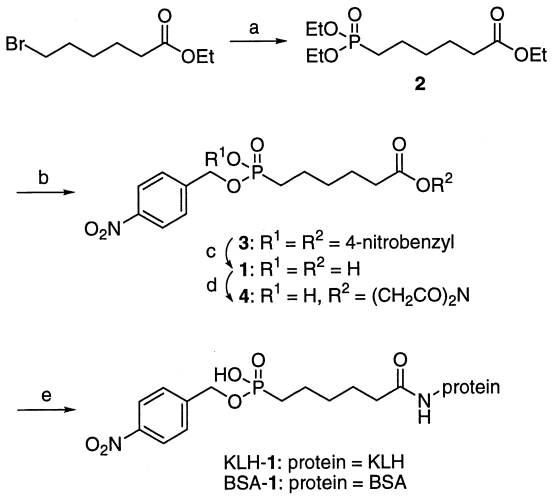

Scheme 1. Synthesis of hapten **1**. Reagents and conditions: a) triethyl phosphite, 155 °C in sealed tube, 84 %. b) i) concd HCl, reflux; ii) *p*-nitrobenzyl alcohol, DCC, 1H-tetrazole, pyridine, CH_2Cl_2, RT, 70 % in 2 steps. c) NaOH (1N), CH_3CN/H_2O, RT, 81 %. d) *N*-hydroxysuccinimide, WSC, DMAP, DMF/CH_3CN, RT, 40 %. e) KLH or BSA, phosphate buffer (pH 7.2)/DMF.

Antibody production and purification: Five Balb/c mice were immunized with KLH-**1**. After two injections of KLH-**1**, the serum immunoglobulin G (IgG) was titrated against BSA-**1** by means of ELISA. The mouse with the highest titer (> 1:51 200) was again immunized with KLH-**1** using the same procedure. Three days after the last injection, the spleen was harvested, and the cells were fused with myeloma cells to prepare hybridomas using a somatic hybridizer.[6] All IgG-producing hybridomas that bound to BSA-**1** were subcloned twice to yield a total of 38 cell lines, which produced monoclonal antibodies. The antibodies were purified from the culture media supernatants by anti-mouse IgG+IgM affinity chromatography.

Catalytic assay and kinetics: The antibodies were screened for the ability to catalyze the hydrolysis of substrate **5** (Table 1). The reaction was performed using antibody (5 μM) and **5** (200 μM) in 10 % DMSO/50 mM Tris-HCl (pH 8.0, 25 °C), and the production of *p*-nitrobenzyl alcohol was monitored by HPLC (absorbance observed at 278 nm). As a result, two antibodies were found to be catalytic. These catalytic antibodies catalyzed the hydrolysis with multiple turnovers and no product inhibition was detected. Of the two catalytic IgG molecules, 7B9 showed greater activity and was chosen for further study. The 7B9-catalyzed hydrolysis of **5** displayed saturation kinetics described by the Michaelis–Menten equation [Eq. (1) - see later].[7] The first-order rate constant (k_{cat})[8] and Michaelis–Menten constant (K_m) are 2.01×10^{-2} min^{-1} and 346 μM, respectively. The observed rate acceleration (k_{cat}/k_{uncat}, where $k_{uncat} = 1.96 \times 10^{-5}$ min^{-1}) was 1020 (Table 1). This antibody-catalyzed reaction was competitively inhibited by hapten **1** ($K_i = 31.1$ nM), and this demonstrates that the catalytic activity is associated with binding in the antibody-combining site.

Table 1. Kinetic parameters of antibody 7B9-catalyzed hydrolyses of esters **5**, **6**, and **7**.[a]

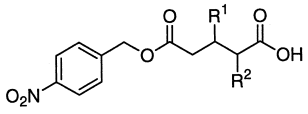

	R^1	R^2	K_m [μM]	k_{cat} [min^{-1}]	k_{cat}/K_m [M^{-1}min^{-1}]	k_{cat}/k_{uncat}
5	H	H	346	2.01×10^{-2}	58.1	1020
6	CH_3	H	456	5.08×10^{-3}	11.1	758
(*R*)-**7**	H	(*R*)-CH_3	223	4.54×10^{-2}	204	1820
(*S*)-**7**	H	(*S*)-CH_3	712	2.01×10^{-2}	28.2	804

[a] Reaction conditions: 10 % DMSO/Tris-HCl (50 mM) (pH 8.0), 25 °C.

Substrate specificity: Since a major goal of this work was to generate antibody catalysts with broad substrate specificity for use as deprotecting reagents, a variety of *p*-nitrobenzyl ester derivatives were examined in the hydrolysis with antibody 7B9. As shown in Tables 1 and 2, antibody 7B9 was able to accept a broad range of *p*-nitrobenzyl esters in addition to the glutaric monoester **5**, which has a structure homologous to that of hapten **1**. The hydrolytic reactions of

Table 2. Kinetic parameters of antibody 7B9-catalyzed hydrolyses of esters **8a–c**.[a]

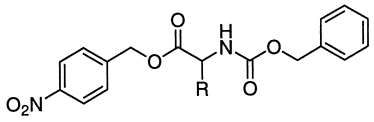

8

	R	K_m [μM]	k_{cat} [min^{-1}]	k_{cat}/K_m [$M^{-1}min^{-1}$]
L-**8a**	$(CH_3)_2CHCH_2$	22.4	1.67×10^{-3}	74.6
D-**8a**	$(CH_3)_2CHCH_2$	10.6	4.68×10^{-4}	44.2
L-**8b**	$CH_3CH_2CH_2CH_2$	13.0	2.15×10^{-3}	165
D-**8b**	$CH_3CH_2CH_2CH_2$	8.5	5.32×10^{-4}	62.5
L-**8c**	$PhCH_2$	4.7	1.83×10^{-3}	389
D-**8c**	$PhCH_2$	1.9	4.00×10^{-4}	211

[a] Reaction conditions: 10% DMSO/Tris-HCl (50 mM) (pH 8.0), 25 °C.

the β- or γ-methyl-substituted *p*-nitrobenzyl glutaric monoesters **6** and **7** were efficiently catalyzed with 7B9, and the β- or γ-methyl substitutions had little effect on the k_{cat} and K_m relative to those observed for **5** (Table 1). Furthermore, 7B9 was found to accept various α-substituted *p*-nitrobenzyl esters, as found using the esters of Leu (**8a**), Norleu (**8b**), and Phe (**8c**). Thus, the antibody is quite tolerant to structural variation, even in the vicinity of the reactive center of the substrates. As shown in Table 2, a comparison between the stereoisomers of α-substituted *p*-nitrobenzyl esters (L-**8a–c** and D-**8a–c**) revealed that 7B9 hydrolyzed both isomers with almost the same values for the specificity constants, k_{cat}/K_m. Since the k_{cat}/K_m value correlates to the stabilization of the transition state, according to transition-state theory,[7] this observation indicates that the antibody stabilizes the transition state of both isomers to a similar extent. On the other hand, if the C_α substituents of *p*-nitrobenzyl esters (**8a–c**) are compared, the increase in the hydrophobicity leads to a decrease in the K_m values that results in an increase in the k_{cat}/K_m values. Together with the tolerance to the stereoisomers, this suggests the existence of nonspecific hydrophobic interactions between the C_α substituents and amino acid residues outside the antigen-combining site, although the details remain unclear at present. These results revealed that the antibody has the potential to be a practical deprotecting reagent that accepts a wide range of *p*-nitrobenzyl ester derivatives as substrates.

Variable-region sequences of antibody 7B9: To construct a three-dimensional model of the antigen-combining site of 7B9, the V-J and V-D-J polypeptide sequences were deduced from the nucleotide sequences (Figure 2). The *c*DNAs of the light- and heavy-chain Fab genes were generated from the hybridoma mRNA by reverse transcription PCR and then were cloned and sequenced. The heavy-chain (Hc) and light-chain (Lc) constant region sequences of 7B9 were found to be the IgG_{2b} and C_κ subclasses, respectively. The sequence analysis of the variable region showed that the heavy and light chains belong to the V_H IIID and V_LV subgroups, respectively.[9] In Figure 2, the amino acid sequences of 7B9 are compared with those of catalytic antibody D2.3, since both antibodies were elicited against similar *p*-nitrobenzyl phosphonates.[10] Interestingly, despite the structural similarity of the immunized haptens, the sequences of 7B9 were different from those of D2.3; the sequence identities in the region of Frame 1 to 3 of the Hc and Lc are 66% and 42%, respectively. In particular, remarkable differences are apparent in the complimentarity-determining region (CDR) 3 of the Hc and CDR 1 of the Lc. Antibody 7B9 possesses nine amino acid residues in the Hc CDR 3 and eleven amino acid residues in the Lc CDR1, while the Hc CDR3 and the

V_H amino acid sequences

```
          10        20        30        40              52        60
                                    CDR1                      CDR2
7B9   PELEKPGASVKISCKASGYSFTDYNMNWVKQSNGKCLEWIGNIDPYYGSTKYNQKFEDKAT
D2.3  A--LR--T---L---T---I--S-WIH----RS-QG----AR-Y-GT---Y--E--KG---

          70        82        90       100              110
                                         CDR3
7B9   LTVDKSSSTAYMQLKSLTSEDSAIYYCVRSNKYTGSV.....YWGQGTTLTVSSAKTTHP
D2.3  --A----------ST-K-----V-F-T-WGFIPVREDYVMD------SV--------A-
```

V_L amino acid sequences

```
          10        20        30        40        50        60
                              CDR1                      CDR2
7B9   SSMSVSLGDTVTITCHASQGIR.....SNIGWLQQKPGKSFKGLIYLGTNLEDEVPSRFS
D2.3  LTL--TI-QPAS-S-KS--SLLYSNGKTYLN--L-R--Q-P-R--H-VSK-DSG--D-IT

          70        80        90       100       110
                                   CDR3
7B9   GSGSGADYSLTISSLESEDFADYYCVQYAQFPRTFGGGTRLEIKRADAAP
D2.3  -----T-FT-K--RV-A--LGV-----GTH--Y------K----------
```

Figure 2. Heavy- and light-chain variable-region deduced polypeptide sequences of antibodies 7B9 and D2.3. CDRs are in boldface type. Dashes indicate identity with the sequence of 7B9 and dots, used to align sequences, represent no amino acid residue at a position. Residue numbering and CDRs are as defined by Kabat et al.[9]

0947-6539/00/0609-1658 $ 17.50+.50/0 *Chem. Eur. J.* **2000**, *6*, No. 9

Lc CDR1 loops of antibody D2.3 are fourteen and sixteen residues long, respectively. The sequence comparison suggests that the antigen-combining sites of 7B9 and D2.3 would have different shapes (vide infra).

Three-dimensional structure model: To understand the observed substrate specificity at a molecular level, a three-dimensional computer model of the antigen-combining site of 7B9 was constructed. The model construction was based on the X-ray crystal structures of the frameworks and the CDR loops with the amino acid sequences homologous to those of antibody 7B9.[11] Thus, the structural coordinates (PDB code: 1fgv and 1fig) of the most homologous framework regions were used as templates for the model of 7B9. The six CDR loops, Lc CDR1, Lc CDR2, Lc CDR3, Hc CDR1, Hc CDR2, and Hc CDR3, were modeled by using the X-ray structures (PDB code: 1eap, 1bbj, 1gaf, 1clo, 1fig, and 7fab, respectively) selected according to the canonical rules.[12, 13] The modeled loops were grafted onto the parent framework structures (1fgv and 1fig). The V_L/V_H interface geometry and the hapten docking to the modeled combining site were based on the coordinates of CNJ206 (PDB code: 1kno),[14] an antibody generated against a *p*-nitrophenyl phosphonate hapten.

The modeled complex with hapten **1** is shown in Figures 3 (left) and 4. The model shows that the hapten is bound in the antigen-combining site with electrostatic and hydrophobic packing interactions. Thus, the *p*-nitrobenzyl moiety of the hapten is buried in a hydrophobic cavity formed by Val^{H37}, Trp^{H47}, Trp^{H103}, and Phe^{L98} (Figure 4). These residues were found to be conserved in the X-ray structures of other hydrolytic antibodies, CNJ206,[14] 48G7,[15] and 17E8,[16] elicited against aryl phosphonate haptens.[17] The observed structural similarity in the hydrophobic pockets is consistent with the concept of "structural convergence",[18] and thus supports the validity of the 7B9 model. The model also indicates that the guanidine group of Arg^{L96}, positioned at the edge of the antigen-combining site, would bind to the phosphorus oxyanion of the hapten by an electrostatic interaction, and this suggests that it participates in the stabilization of the reaction transition state (Figure 4).

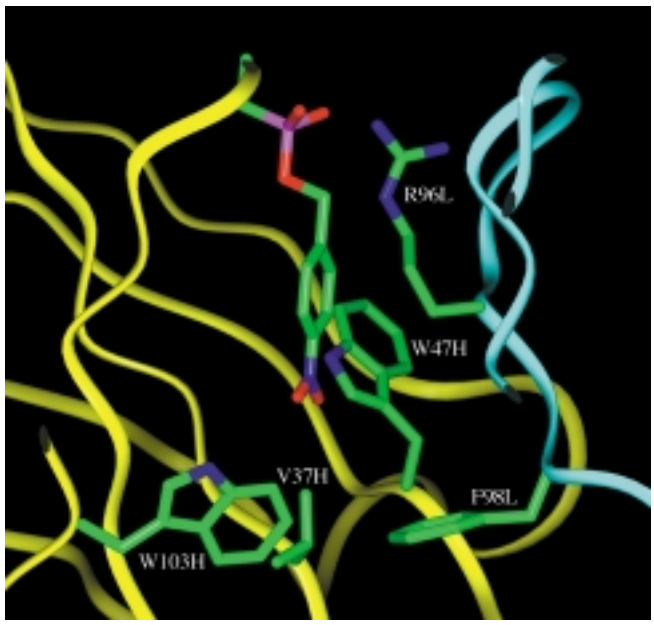

Figure 4. Three-dimensional model of the antigen-combining site of antibody 7B9 complexed with hapten **1**. The heavy and light chains are shown with yellow and blue ribbons, respectively. The amino acid residues are labeled with their single-letter notation, and are numbered according to Kabat et al.[9] Hapten **1** and the labeled amino acid side chains are colored according to the atoms: carbon is green, nitrogen is blue, oxygen is red, and phosphorus is magenta.

Comparison between antibodies 7B9 and D2.3: As described above, the catalytic antibody D2.3 was elicited against the

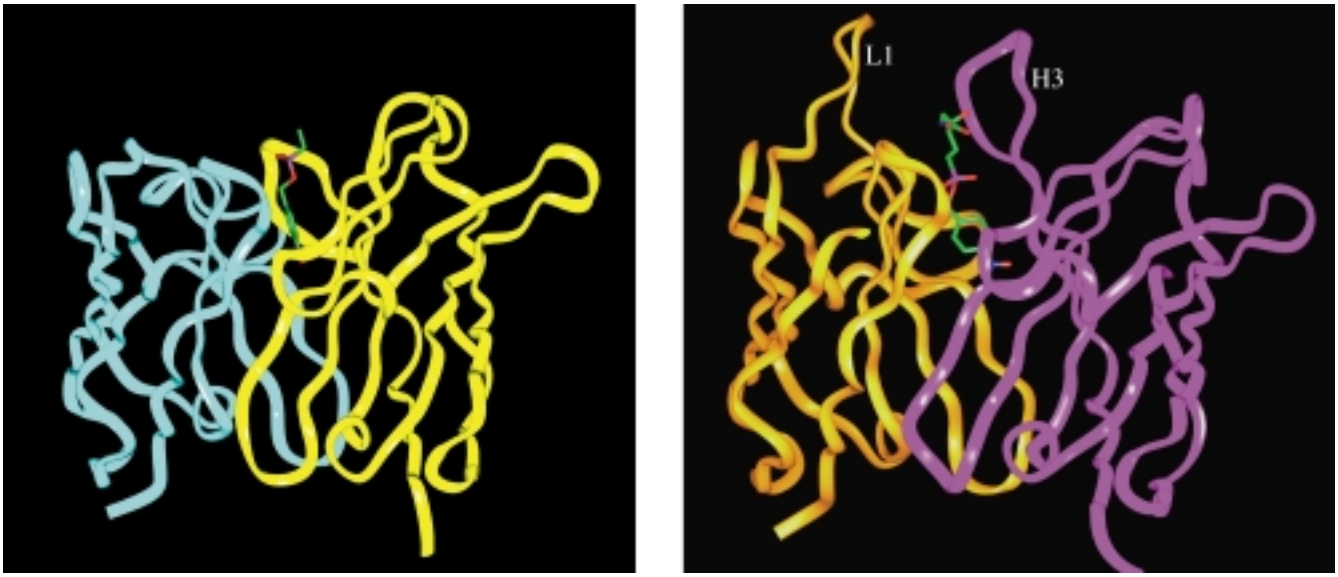

Figure 3. Left) Three-dimensional model of the complex of antibody 7B9 (Fv) with hapten **1**. The heavy and light chains are shown with yellow and blue ribbons, respectively. Hapten **1** is colored according to the atoms: carbon is green, nitrogen is blue, oxygen is red, and phosphorus is magenta. Right) The X-ray structure of antibody D2.3 complexed with the hapten (PDB code: 1yec). The heavy and light chains are shown with purple and orange ribbons, respectively. The hapten is colored in the same manner as the figure on the left.

hapten **9**, which is structurally homologous to that for 7B9. However, the structural and functional characteristics of antibody D2.3 are considerably different from those of 7B9. In fact, broad substrate specificity was observed in 7B9 but

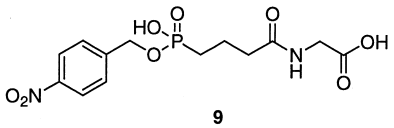

9

not in D2.3.[10] Although the residues that form the hydrophobic cavity at the bottom of the antigen-combining site in D2.3 are also found in 7B9, the global shapes of the antigen-combining sites are totally different in 7B9 and D2.3 (PDB code: 1yec), as shown in Figure 3. Since D2.3 possesses Lc CDR1 and Hc CDR3 loops, which are five residues longer than those of 7B9, respectively, the loops extend outside to form the walls of the antigen-combining site. Thus, the antigen-combining site of D2.3 forms a relatively deep cavity with these extended loops, in which two hydrogen bonds are observed between the *N*-glutarylglycinate part of the hapten and the Fab of D2.3 (Figure 3, right). On the other hand, 7B9 possesses no extended loops that result in the relatively shallow binding pocket (Figure 3, left). The model of 7B9 complexed with the hapten shows that there is no pocket to accommodate any moiety other than the *p*-nitrobenzyl phosphonate in the combining site. These findings are consistent with the observed broad substrate specificity of 7B9. In the antibody-catalyzed hydrolysis, the α-, β-, and γ-substituents of the substrates should be outside the combining site and ignored in the antibody recognition.

Since small molecules are not immunogenic unless coupled to a carrier protein, methylene tethers were incorporated into the phosphonate transition-state analogues in order to couple the haptens to the carrier proteins. Thus far, little attention has been paid to the linker moieties in hapten design for the generation of catalytic antibodies. However, as shown above, the comparison between antibodies 7B9 and D2.3 suggests that the linker moiety of the haptens plays an important role in the control of substrate specificity. Although the only difference between the haptens of 7B9 and D2.3 is the linker moiety between the *p*-nitrobenzyl phosphonate and the carrier protein, it seems to affect the modes of the antibody–antigen interactions considerably. In the generation of 7B9, the suitable length of the linker precludes any steric interference with the carrier side chains and then enhances the selectivity of the antibody for the *p*-nitrobenzyl phosphonate. In addition, the unsubstituted alkyl chain of the linker does not interact with the amino acids in the antigen-combining site. These characteristics would induce the construction of the relatively shallow binding pocket of antibody 7B9.

Conclusion

In this work, we have reported the generation of an antibody that hydrolyzes a wide range of α-, β-, and γ-substituted *p*-nitrobenzyl esters. This catalytic antibody would be useful for removal of the *p*-nitrobenzyl protective group of carboxylic acids, especially in cases where the conventional chemical and enzymatic methods are not suitable. However, in terms of catalytic efficiency, 7B9 must be improved to have a k_{cat} of about 2 min^{-1}; this should be achieved by directed evolution on phage-displayed libraries[19] or site-directed mutagenesis.[20] The structural investigations of the antigen-combining site suggest that the linker moiety of haptens plays an important role in the control of substrate specificity. The further studies of antibodies with the same hapten design would extend the scope of protective-group removal with catalytic antibodies.

Experimental Section

General methods (synthesis): All oxygen- or moisture-sensitive reactions were carried out under argon. Analytical chromatography was performed on silica gel 60 F_{254} plates (0.25 mm) (Merck). Preparative thin-layer chromatography (TLC) was performed on silica gel 60 F_{254} plates (0.5 mm) (Merck). Flash chromatography was performed on silica gel 60 (230–400 mesh) (Merck). High-performance liquid chromatography (HPLC) was performed on a Hitachi L6200 equipped with an L4200 UV detector. ^{1}H and ^{13}C NMR spectra were recorded on a Bruker DPX300 (300 MHz) NMR spectrometer. The spectra were reported in δ downfield from tetramethylsilane. Melting points were determined with a Yanagimoto melting point apparatus and were not corrected. Infrared spectra were recorded on a SHIMADZU 8000 Series FTIR spectrometer. Optical rotations were measured on a HORIBA SEPA300 polarimeter. Mass spectra were obtained on JEOL JMS-SX/SX102A and JEOL JMS-AX505H mass spectrometers.

Ethyl 6-(diethoxyphosphoryl)hexanoate (2): A mixture of triethyl phosphite (9.20 mL, 53.7 mmol) and ethyl 6-bromocaproate (3.17 mL, 17.9 mmol) was stirred at 155 °C for 12 h in a sealed tube. The resulting product was distilled under reduced pressure to afford the desired product **2** (135 °C/1.5 mm Hg, 4.23 g, 84 %) as a colorless oil. IR (film): $\tilde{\nu}$ = 1732, 1240 cm^{-1}; ^{1}H NMR (300 MHz, CD_3OD): δ = 4.17–4.03 (m, 6H), 2.32 (t, J = 7.3 Hz, 2H), 1.78 (m, 2H), 1.62 (m, 4H), 1.44 (m, 2H), 1.32 (t, J = 7.1 Hz, 6H), 1.24 (t, J = 7.1 Hz, 3H); ^{13}C NMR (75 MHz, CD_3OD): δ = 175.2, 63.1 (J_{CP} = 6.7 Hz), 61.4, 34.8, 30.8 (J_{CP} = 16.2 Hz), 26.6, 25.5, 23.1 (J_{CP} = 5.2 Hz), 16.7 (J_{CP} = 5.9 Hz), 14.5; HRMS (FAB^+): calcd for $C_{12}H_{26}O_5P$ $[M+H]^+$ 281.1518; found 281.1523.

4-Nitrobenzyl 6-[bis(4-nitrobenzyloxy)phosphoryl]hexanoate (3): A solution of **2** (52.2 mg, 0.186 mmol) in concentrated HCl (4.0 mL) was refluxed with stirring for 15 h. The solvent was removed in vacuo. *p*-Nitrobenzyl alcohol (144.0 mg, 0.940 mmol), *N*,*N*′-dicyclohexyl carbodiimide (DCC) (211 mg, 1.03 mmol), and 1H-tetrazole (13.1 mg, 0.187 mmol) were added to a stirred solution of the resulting residue in CH_2Cl_2 (2.0 mL) and pyridine (0.5 mL) at room temperature. After stirring for 18 h, the mixture was filtered. The filtrate was concentrated in vacuo, and the obtained residue was purified by HPLC (YMC AM323: C-18 reverse-phase column, ϕ 10 mm × 250 mm, CH_3CN/0.1 % aqueous trifluoroacetic acid (TFA) = 70:30, 3.0 mL min^{-1}, 254 nm, retention time 12.1 min). The CH_3CN and TFA were removed in vacuo, and the water was removed by lyophilization to give **3** as a white solid (78.8 mg, 70 %). IR (film): $\tilde{\nu}$ = 1738, 1607, 1526, 1348, 1244 cm^{-1}; ^{1}H NMR (300 MHz, $CDCl_3$): δ = 8.21 (d, J = 8.7 Hz, 6H), 7.51 (d, J = 8.7 Hz, 6H), 5.22–5.06 (m, 4H), 5.20 (s, 2H), 2.38 (t, J = 7.3 Hz, 2H), 1.91–1.80 (m, 2H), 1.70–1.60 (m, 4H), 1.46–1.40 (m, 2H); ^{13}C NMR (75 MHz, $CDCl_3$): δ = 172.8, 147.8, 147.6, 143.2 (J_{CP} = 3.2 Hz), 143.1, 128.3, 127.9, 123.8, 123.7, 65.7 (J_{CP} = 6.2 Hz), 64.6, 33.6, 29.7 (J_{CP} = 16.9 Hz), 26.6, 24.7, 21.9 (J_{CP} = 5.2 Hz); HRMS (FAB^+): calcd for $C_{27}H_{29}O_{11}N_3P$ $[M+H]^+$ 602.1540; found 602.1533.

6-[Hydroxy(4-nitrobenzyloxy)phosphoryl]hexanoic acid (hapten 1): NaOH (1N, 0.50 mL, 0.50 mmol) was added to a solution of **3** (24.5 mg, 0.041 mmol) in CH_3CN (0.5 mL) and H_2O (0.5 mL) at room temperature. After stirring for 10 h, the reaction mixture was acidified with HCl (2N) and purified by HPLC (YMC AM323: C-18 reverse-phase column, ϕ 10 mm × 250 mm, CH_3CN /0.1 % aqueous TFA = 35:65, 3.0 mL min^{-1}, 254 nm, retention time 8.7 min). The CH_3CN and TFA were removed in vacuo,

0947-6539/00/0609-1660 $ 17.50+.50/0 *Chem. Eur. J.* **2000**, *6*, No. 9

and the water was removed by lyophilization to give **1** as a white solid (10.9 mg, 81%). IR (film): $\tilde{\nu}$ = 1723, 1696, 1615, 1543, 1526 cm^{-1}; ^{1}H NMR (300 MHz, CD_3OD): δ = 8.25 (d, J = 8.7 Hz, 2H), 7.64 (d, J = 8.7 Hz, 2H), 5.14 (d, J = 7.9 Hz, 2H), 2.28 (t, J = 7.2 Hz, 2H), 1.86–1.37 (m, 8H); ^{13}C NMR (75 MHz, CD_3OD): δ = 177.3, 149.1, 145.9 (J_{CP} = 6.5 Hz), 129.1, 124.6, 66.2 (J_{CP} = 5.9 Hz), 34.6, 31.0 (J_{CP} = 16.3 Hz), 27.6, 25.8, 23.4 (J_{CP} = 5.1 Hz); HRMS (FAB$^+$): calcd for $C_{13}H_{19}O_7NP$ $[M+H]^+$ 332.0899; found 332.0916.

Succinimidyl 6-[hydroxy(4-nitrobenzyloxy)phosphoryl]hexanoate (4): A mixture of **1** (31.8 mg, 0.096 mmol), *N*-hydroxysuccinimide (13.2 mg, 0.115 mmol), WSC 1-(3-dimethylaminopropyl)-3-ethylcarbodiimide hydrochloride (22.0 mg, 0.115 mmol), and 4-dimethylaminopyridine (3.5 mg, 0.029 mmol) in DMF (0.5 mL) and CH_3CN (1.5 mL) was stirred at room temperature for 17 h. The reaction mixture was acidified with HCl (2N) and purified by HPLC (YMC AM323: C-18 reverse-phase column, ϕ 10 mm × 250 mm, CH_3CN /0.1% aqueous TFA = 37:63, 3.0 mL min^{-1}, 254 nm, retention time 11.3 min). The CH_3CN and TFA were removed in vacuo, and the water was removed by lyophilization to give **4** as a white solid (16.3 mg, 40%). IR (film): $\tilde{\nu}$ = 1738, 1723, 1700, 1605, 1526 cm^{-1}; ^{1}H NMR (300 MHz, CD_3OD): δ = 8.25 (d, J = 8.7 Hz, 2H), 7.64 (d, J = 8.7 Hz, 2H), 5.15 (d, J = 8.0 Hz, 2H), 2.83 (s, 4H), 2.62 (t, J = 7.2 Hz, 2H), 1.88–1.50 (m, 8H); HRMS (FAB$^+$): calcd for $C_{17}H_{21}O_9N_2PNa$ $[M+Na]^+$ 451.0882; found 451.0876.

KLH-1: A KLH solution in Na_2HPO_4-NaH_2PO_4 (200 mM, pH 7.2, 9.66 mg mL^{-1}, 1450 μL) at room temperature was added to a stirred solution of **4** (4.0 mg, 0.0093 mmol) in DMF (150 μL) and Na_2HPO_4-NaH_2PO_4 (200 mM, pH 7.2, 400 μL). After 19 h, the mixture was purified by Sephadex G 25M chromatography (Pharmacia, PD-10) (PBS buffer) to give **KLH-1**. The concentration of **KLH-1** was determined by bicinchoninic acid (BCA) protein assay[21] (6.7 mg mL^{-1}).

BSA-1: A BSA solution in Na_2HPO_4-NaH_2PO_4 (200 mM, pH 7.2, 10.8 mg in 560 μL) at room temperature was added to a stirred solution of **4** (4.2 mg, 0.0097 mmol) in DMF (150 μL) and Na_2HPO_4-NaH_2PO_4 (200 mM, pH 7.2, 790 μL). After 19 h, the mixture was purified by Sephadex G-25M chromatography (Pharmacia, PD-10) (PBS buffer) to give BSA-**1**. The concentration of BSA-**1** was determined by BCA protein assay[21] (0.6–7.3 mg mL^{-1}, four fractions).

Mono(4-nitrobenzyl) glutarate (5): A solution of *p*-nitrobenzyl alcohol (2.16 g, 14.1 mmol), glutaric anhydride (2.42 g, 21.2 mmol), and triethylamine (5.00 mL, 35.9 mmol) in CH_3CN (25 mL) was stirred at room temperature. After 15 h, the reaction mixture was poured into aqueous $KHSO_4$ (5%) and was extracted with EtOAc. The combined organic layers were washed with brine, dried over Na_2SO_4, and concentrated in vacuo. The residue was purified by flash chromatography (SiO_2, $CHCl_3$ to 40:1 $CHCl_3$:MeOH) to give **5** as colorless crystals (3.73 g, 98%). M.p. 72–74 °C; IR (film): $\tilde{\nu}$ = 3480, 1709, 1605, 1522 cm^{-1}; ^{1}H NMR (300 MHz, $CDCl_3$): δ = 8.22 (d, J = 8.8 Hz, 2H), 7.52 (d, J = 8.8 Hz, 2H), 5.22 (s, 2H), 2.51 (t, J = 7.3 Hz, 2H), 2.46 (t, J = 7.2 Hz, 2H), 2.00 (m, 2H); ^{13}C NMR (75 MHz, $CDCl_3$): δ = 178.9, 172.3, 147.7, 143.1, 128.3, 123.7, 64.8, 32.9, 32.8, 19.6; HRMS (FAB$^+$): calcd for $C_{12}H_{14}O_6N$ $[M+H]^+$ 268.0822; found 268.0814.

Mono(4-nitrobenzyl) 3-methylglutarate (6): A solution of *p*-nitrobenzyl alcohol (934 mg, 6.10 mmol), 3-methylglutaric anhydride (1.02 g, 8.00 mmol), and triethylamine (2.55 mL, 18.3 mmol) in CH_3CN (22 mL) was stirred at room temperature. After 7 h, the reaction mixture was poured into aqueous $KHSO_4$ (5%) and was extracted with EtOAc. The combined organic layers were washed with brine, dried over Na_2SO_4, and concentrated in vacuo. The residue was purified by flash chromatography (SiO_2, $CHCl_3$ to 60:1 $CHCl_3$:MeOH) to give **6** as a white solid (1.66 g, 97%). M.p. 65–67 °C; IR (film): $\tilde{\nu}$ = 3114, 1740, 1709, 1609, 1522 cm^{-1}; ^{1}H NMR (300 MHz, $CDCl_3$): δ = 8.23 (d, J = 8.7 Hz, 2H), 7.52 (d, J = 8.7 Hz, 2H), 5.22 (s, 2H), 2.55–2.28 (m, 5H), 1.07 (d, J = 6.2 Hz, 3H); ^{13}C NMR (75 MHz, $CDCl_3$): δ = 178.4, 171.8, 147.7, 143.1, 128.4, 123.7, 64.7, 40.4, 40.3, 27.1, 19.8; HRMS (FAB$^+$): calcd for $C_{13}H_{16}O_6N$ $[M+H]^+$ 282.0978; found 282.0986.

1-Mono(4-nitrobenzyl) (4*R*)-4-methylglutarate ((*R*)-7): A solution of *p*-nitrobenzyl alcohol (1.01 g, 6.58 mmol), (*R*)-(+)-2-methylglutaric acid (1.46 g, 9.97 mmol), WSC (1.46 g, 7.59 mmol), and 4-dimethylaminopyridine (364 mg, 2.98 mmol) in CH_3CN (65 mL) was stirred at room temperature. After 36 h, the reaction solvent was removed in vacuo. The residue was poured into aqueous $KHSO_4$ (5%) and was extracted with EtOAc. The combined organic layers were washed with brine, dried over Na_2SO_4, and concentrated in vacuo. A small portion of pure **(*R*)-7** (R_f 0.50 in 20:1 $CHCl_3$:MeOH, colorless crystals) was obtained by flash chromatography (SiO_2, $CHCl_3$ to 80:1 $CHCl_3$:MeOH), but another regioisomer, 1-mono(4-nitrobenzyl) (2*R*)-2-methyl glutarate (R_f 0.45 in 20:1 $CHCl_3$:MeOH), could not be isolated from the mixture, even by HPLC (YMC AM323: C-18 reverse-phase column, ϕ 10 mm × 250 mm; YMC-SIL A023: normal-phase column, ϕ 10 mm × 250 mm). The structure of **(*R*)-7** was unambiguously differentiated from that of the regioisomer by heteronuclear multiple-quantum coherence (HMQC) and heteronuclear multiple-bond correlation (HMBC) measurements. **(*R*)-7**: M.p. 65–67 °C; $[\alpha]_D^{25} = -14.5$ (c = 0.61 in $CHCl_3$); IR (film): $\tilde{\nu}$ = 3100, 1734, 1705, 1609, 1522 cm^{-1}; ^{1}H NMR (300 MHz, $CDCl_3$): δ = 8.23 (d, J = 8.7 Hz, 2H), 7.51 (d, J = 8.7 Hz, 2H), 5.21 (s, 2H), 2.61–2.41 (m, 3H), 2.03 (m, 1H), 1.84 (m, 1H), 1.23 (d, J = 7.0 Hz, 3H); ^{13}C NMR (75 MHz, $CDCl_3$): δ = 181.8, 172.5, 147.7, 143.1, 128.4, 123.8, 64.8, 38.5, 31.6, 28.1, 16.9; HRMS (FAB$^+$): calcd for $C_{13}H_{16}O_6N$ $[M+H]^+$ 282.0978; found 282.0986.

1-Mono(4-nitrobenzyl) (2*R*)-2-methyl glutarate: ^{1}H NMR (300 MHz, $CDCl_3$): δ = 8.23 (d, J = 8.6 Hz, 2H), 7.52 (d, J = 8.6 Hz, 2H), 5.22 (s, 2H), 2.62 (m, 1H), 2.43–2.38 (m, 2H), 2.02 (m, 1H), 1.82 (m, 1H), 1.23 (d, J = 7.1 Hz, 3H).

1-Mono(4-nitrobenzyl) (4*S*)-4-methylglutarate ((*S*)-7): **(*S*)-7** was prepared in the same manner as described above using (*S*)-(−)-2-methylglutaric acid, and a small portion of pure **(*S*)-7** (colorless crystals) was obtained by flash chromatography (SiO_2, $CHCl_3$ to 80:1 $CHCl_3$:MeOH). $[\alpha]_D^{25} = +15.1$ (c = 1.0 in $CHCl_3$).

Antibody production and purification: Five Balb/c mice each received an intraperitoneal injection of KLH-**1** conjugate (100 μg) emulsified in RIBI adjuvant (MPL and TDM emulsion) on days 1 and 14 (boost #1). On day 21, serum was taken from the mice, and the titer was determined by ELISA. On day 42, the mouse with the highest titer received a second intraperitoneal boost (boost #2) with KLH-**1** conjugate. Three days after the last boost (boost #2), the spleen was taken from the mouse, and the cells were fused with 5×10^7 P3X63-Ag8.653 myeloma cells by a Shimadzu Somatic Hybridizer SSH 10 (electrode distance: 1.0 mm; frequency: 1 MHz; primary AC voltage: 80 V; initial time: 10 s; pulse width: 40 ms; DC voltage: 920 V; electric field strength: 2.30 kV cm^{-1}; secondary AC voltage: 80 V; pulse repeat interval: 1 s; number of pulses: 1; VDC change: +0 V; final time: 10 s; AC voltage decrease rate: 0%; adhesion intensifier: off). Hybridoma cells were plated into seven 96-well plates; each well contained HAT-RPMI 1640 (100 μL) with fetal bovine serum (20%) and Briclone (5%, BioResearch Ireland). After two weeks, the plates were analyzed by ELISA for binding to the BSA-**1** conjugate. All positive colonies were subcloned twice according to the standard protocols. All cell lines that retained active binding after subcloning were individually grown to 200 mL, and the supernatants were purified by anti-mouse IgG + IgM affinity chromatography (NGK Industries; loaded on in PBS and eluted with 0.2M glycine-HCl, pH 2.5) to yield purified antibodies. The antibodies were judged to be homogeneous (>95%) by sodium dodecylsulfate/polyacrylamide gel electrophoresis (SDS-PAGE). The subclass of each antibody was determined by using a monoclonal isotyping kit purchased from Amersham (RPN 29).

Catalytic assays and kinetic measurements: Purified monoclonal antibodies were dialyzed against Tris-HCl (50 mM, pH 8.0), and for the initial assay of catalytic activity, the antibody concentrations were determined by measuring the absorbance at 280 nm. Reactions were initiated by the addition of a stock solution (10 μL) of substrate in DMSO to antibody solution (90 μL) in Tris-HCl (50 mM, pH 8.0 at 25 °C). Hydrolysis rates were measured by HPLC detection of *p*-nitrobenzyl alcohol with injection (10 μL) of the reaction mixture. The analytical HPLC was performed on a Hitachi L6200 unit equipped with a Hitachi L4000 UV detector, using a YMC ODS AM 303 column eluted with acetonitrile/aqueous TFA (0.1%, 35:65) at a flow rate of 1.0 mL min^{-1} with detection at 278 nm. The retention time of *p*-nitrobenzyl alcohol was 7.0 min. Initial rates were determined from the linear range of the rate. The observed rate was corrected for the uncatalyzed rate of hydrolysis in the absence of antibody. The kinetic parameters, k_{cat} and K_m, were determined by nonlinear least-squares fitting of the initial rate against substrate concentration to a hyperbolic curve described by the Michaelis–Menten equation [Eq. (1)].

$$v = k_{cat}[Ab][S]/(K_m + [S]) \quad (1)$$

In this equation, v is the initial velocity, [Ab] is the active site concentration of the antibody obtained from the activity assay (see below), and [S] is the substrate concentration.[7] The background rates (k_{uncat}) were determined in the absence of antibody under otherwise identical conditions.

Active-site titration and inhibition assay: The active-site concentration of the catalytic antibody and the inhibition constant K_i for hapten **1** were determined by quantitating the effect of the concentration of **1** on the velocity of the antibody-catalyzed hydrolysis of substrate **5**. Rates obtained at fixed antibody and substrate concentrations were fitted to the following equation [Eq. (2)].

$$v = \{(v_0/2E)[E - I - K_i' + (I + K_i' - E)^2 + 4EK_i']^{1/2}\} \quad (2)$$

In the equation, $K_i' = K_i(1 + [S]/K_m)$, and v is the initial rate in the presence of **1**, v_0 is the initial rate in the absence of **1**, E is the concentration of functional catalysis, I is the concentration of **1**, K_i' is the apparent inhibition constant, and [S] is the substrate concentration.[22]

***c*DNA synthesis, cloning, and nucleotide sequence analysis**: Total RNA was isolated from 10^7 hybridoma cells using the RNeasy Mini kit (QIAGEN). First-strand *c*DNA was synthesized from the isolated total RNA using the RT-PCR kit with oligo (dT) primer (Stratagene). The Fd fragment- and light-chain (κ)-encoding regions were amplified by PCR under the standard conditions using *Ex Taq* polymerase (Takara, Japan) and the following primers: Fd sequence-specific primers (up: 5′-AGGTC-CAGCTGCTCGAGTCTGG-3′, down: 5′-AGGCTTACTAGTGTGA-CACTCCTTGCATGG-3′), or κ sequence-specific primers (up: 5′-CCAGATGTGAGCTCGTGATGACCCAGACTCCA-3′, down: 5′-GCGCCGTCTAGAATTAACACTCATTCCTGTTGAA-3′). The Fd and κ amplified fragments were digested with *Xho* I/*Spe* I and *Sac* I/*Xba* I, respectively, and ligated sequentially into the appropriately digested vector, pComb3.[23] Nucleotide sequencing was carried out using a Taq Dye Deoxy Terminator Cycle Sequencing kit (Applied Biosystems) with the primer (5′-AGGGGCCAGTGGATAGAC-3′) for V_H, and the C_κ primer (5′-AACTGCTCACTGGATGG-3′) for V_L.

Molecular modeling: The model of 7B9 was constructed on Insight II.[24] H52 (1fgv) and 1F7 (1fig) were used as the starting structures for the frameworks of V_L and V_H, respectively, due to their amino acid sequence homology. For the five CDR loops (L1, L2, L3, H1, and H2), each canonical structure was determined according to the canonical rules.[12] Then, 17E8 (1eap) for L1, B72.3 (1bbj) for L2, 48G7 (1gaf) for L3, A5B7 (1clo) for H1, and 1F7 (1fig) for H2, which is the same as the starting structure for the framework of V_H, were selected as the starting structures. Recently, the canonical rule for the CDR-H3 loop was established.[13] According to the rule, NEW (7fab) was used as the starting structure for the H3 loop. The amino acid residues of the starting structures for each CDR loop, which were not conserved, were replaced with those of 7B9. The modeled loops were sequentially grafted onto each parent framework structure (H52 and 1F7) by superimposing the backbone atoms (N, C_α, C, and O) of the five residues that precede the loop and the five residues after the loop onto the corresponding atoms of the parent framework structure. The coordinates of CNJ206 (1kno)[14] were chosen as the template to determine the V_L/V_H interface geometry for the following reason. The conserved amino acid residues in the hydrolytic antibodies D2.3, CNJ206, 48G7, and 17E8, which form a hydrophobic cavity at the bottom of the antigen-combining site for a haptenic aryl moiety, are also conserved in antibody 7B9. Among the candidates, the lengths of the CDR loops of CNJ206 are almost the same as those of 7B9 (only the H3 loop is one residue longer), whereas D2.3 has L1 and H3 loops that are five residues longer than those of 7B9, respectively, in spite of it possessing the most similar haptenic structure. Thus, the backbone atoms of the frame regions (FRs) 1, 2, 3, and 4 of 7B9 were superimposed onto the corresponding atoms of CNJ206. Rotamers of the mutated amino acid residues were checked and set to new ones if the side chain contacted the other amino acids. The entire structure was optimized by minimizing the conformational energy with the program PRESTO.[25] The hapten was docked with the modeled combining site by superimposing the hapten of 7B9 onto that of CNJ206 in the complexed X-ray structure.

[1] a) R. A. Lerner, S. J. Benkovic, P. G. Schultz, *Science* **1991**, *252*, 659; b) P. G. Schultz, R. A. Lerner, *Science* **1995**, *269*, 1835.

[2] a) Y. Iwabuchi, H. Miyashita, R. Tanimura, K. Kinoshita, M. Kikuchi, I. Fujii, *J. Am. Chem. Soc.* **1994**, *116*, 771; b) F. Tanaka, K. Kinoshita, R. Tanimura, I. Fujii, *J. Am. Chem. Soc.* **1996**, *118*, 2332; c) T. Li, S. Hilton, K. D. Janda, *J. Am. Chem. Soc.* **1995**, *117*, 2123; d) R. Hirschmann, A. B. Smith III, C. M. Taylor, P. A. Benkovic, S. D. Taylor, K. M. Yager, P. A. Sprengeler, S. J. Benkovic, *Science* **1994**, *265*, 234.

[3] B. L. Iverson, K. E. Cameron, G. K. Jahangiri, D. S. Pasternak, *J. Am. Chem. Soc.* **1990**, *112*, 5320.

[4] T. W. Greene, P. G. M. Wuts, *Protective Groups in Organic Synthesis*, Wiley, New York, **1991**, p. 224.

[5] T. Miyadera, Y. Sugimura, T. Hashimoto, T. Tanaka, K. Iino, T. Shibata, S. Sugawara, *J. Antibiot.* **1983**, *36*, 1034.

[6] a) G. Köhler, C. Milstein, *Nature* **1975**, *256*, 495; b) M. M. S. Lo, T. Y. Tsong, M. K. Conrad, S. M. Strittmatter, L. D. Hester, D. H. Snyder, *Nature* **1984**, *310*, 792.

[7] A. Fersht, *Enzyme Structure and Mechanism*, Freeman, New York, **1985**, p. 98.

[8] The k_{cat}'s were obtained by dividing by measured active site concentrations. The active site concentrations were determined by activity titrations with phosphonate **1** as an inhibitor. See Experimental Section for details.

[9] E. A. Kabat, T. T. Wu, H. M. Perry, K. S. Gottesman, C. Foeller, *Sequences of Proteins of Immunological Interest*, 5th ed., US Department of Health and Human Services NIH, Bethesda, MD, **1991**.

[10] D. S. Tawfik, B. S. Green, R. Chap, M. Sela, Z. Eshhar, *Proc. Natl. Acad. Sci. USA* **1993**, *90*, 373.

[11] The Protein Data Bank (Brookhaven National Laboratories) was accessed for three-dimensional structural information of the templates used in the modeling studies. See text for each accession code.

[12] B. Al-Lazikani, A. M. Lesk, C. Chothia, *J. Mol. Biol.* **1997**, *273*, 927.

[13] a) H. Shirai, A. Kidera, H. Nakamura, *FEBS Lett.* **1996**, *399*, 1; b) V. Morea, A. Tramontano, M. Rustici, C. Chothia, A. M. Lesk, *J. Mol. Biol.* **1998**, *275*, 269; c) B. Oliva, P. A. Bates, E. Querol, F. X. Aviles, M. J. E. Sternberg, *J. Mol. Biol.* **1998**, *279*, 1193.

[14] R. Zemel, D. G. Schindler, D. S. Tawfik, Z. Eshhar, B. S. Green, *Mol. Immunol.* **1994**, *31*, 127.

[15] S. A. Lesley, P. A. Patten, P. G. Schultz, *Proc. Natl. Acad. Sci. USA* **1993**, *90*, 1160.

[16] J. Guo, W. Huang, T. S. Scanlan, *J. Am. Chem. Soc.* **1994**, *116*, 6062.

[17] G. MacBeath, D. Hilvert, *Chem. Biol.* **1996**, *3*, 433.

[18] a) J.-B. Charbonnier, B. Golinelli-Pimpaneau, B. Gigant, D. S. Tawfik, R. Chap, D. G. Schindler, S.-H. Kim, B. S. Green, Z. Eshhar, M. Knossow, *Science* **1997**, *275*, 1140; b) B. Gigant, J.-B. Charbonnier, Z. Eshhar, B. S. Green, M. Knossow, *Proc. Natl. Acad. Sci. USA* **1997**, *94*, 7857.

[19] I. Fujii, S. Fukuyama, Y. Iwabuchi, R. Tanimura, *Nature Biotechnol.* **1998**, *16*, 463.

[20] H. Miyashita, T. Hara, R. Tanimura, S. Fukuyama, C. Cagnon, A. Kohara, I. Fujii, *J. Mol. Biol.* **1997**, *267*, 1247.

[21] P. K. Smith, R. I. Krohn, G. T. Hermanson, A. K. Mallia, F. H. Gartner, M. D. Provenzano, E. K. Fujimoto, N. M. Goeke, B. J. Olson, D. C. Klenk, *Anal. Biochem.* **1985**, *150*, 76.

[22] J. W. Williams, J. F. Morrison, *Methods Enzymol.* **1979**, *63*, 437.

[23] C. F. Barbas, A. S. Kang, R. A. Lerner, S. J. Benkovic, *Proc. Natl. Acad. Sci. USA* **1991**, *88*, 7978.

[24] Pharmacopeia (Molecular Simulations).

[25] K. Morikami, T. Nakai, A. Kidera, M. Saito, H. Nakamura, *Comput. Chem.* **1992**, *16*, 243.

Received: September 13, 1999 [F2029]